

CONF.  
790423--7

LA-UR-79-811

**TITLE:** MEASUREMENT AND ANALYSIS OF DRAG IN  
MULTIPHASE FLOW SYSTEMS

**AUTHOR(S):** P. E. Rexroth  
V. S. Starkovich

**SUBMITTED TO:** 2nd Multi-Phase Flow and Heat Transfer  
Symposium Workshop  
April 16-18, 1979  
Miami Beach, Florida

**NOTICE**  
This report was prepared as an account of work sponsored by the United States Government. Neither the United States nor the United States Department of Energy, nor any of their employees, nor any of their contractors, subcontractors, or their employees, makes any warranty, express or implied, or assumes any legal liability or responsibility for the accuracy, completeness, or usefulness of any information, apparatus, product, or process disclosed, or represents that its use would not infringe privately owned rights.

By acceptance of this article, the publisher recognizes that the U.S. Government retains a non-exclusive, royalty-free license to publish or reproduce the published form of this contribution, or to allow others to do so, for U.S. Government purposes.

The Los Alamos Scientific Laboratory requests that the publisher identify this article as work performed under the auspices of the Department of Energy.

**MASTER**

**MASTL**

  
**Los Alamos**  
**scientific laboratory**  
of the University of California  
LOS ALAMOS, NEW MEXICO 87545

An Affirmative Action/Equal Opportunity Employer

DISTRIBUTION OF THIS DOCUMENT IS UNLIMITED

Form No. 836 R2  
Sl. No. 2629  
1/78

DEPARTMENT OF ENERGY  
CONTRACT W-7405-ENG. 38

EXB

DISTRIBUTION OF THIS DOCUMENT IS UNLIMITED

## MEASUREMENT AND ANALYSIS OF DRAG IN MULTIPHASE FLOW SYSTEMS

P. E. Rexroth and V. S. Starkovich  
Energy Division  
Los Alamos Scientific Laboratory  
University of California  
P. O. Box 1663  
Los Alamos, NM 87545 USA

### ABSTRACT

Presented here is a combined experimental and analytical program undertaken to evaluate an interfield momentum coupling model used in the computer code SIMMER. The behavior of a slugging, vapor-particle flow system was observed and recorded using gamma densitometry, differential pressure measurement, and motion pictures. The primary parameter observed was slug period. When the system was modeled using SIMMER, the calculated behavior of the flow was qualitatively similar to that observed experimentally, but both the period and maximum slug height were underestimated, indicating too weak coupling between the vapor and particle fields. The SIMMER drag correlation was modified, resulting in much better agreement. Final discrepancies between experiment and analysis are discussed.

### INTRODUCTION

SIMMER[1] (for S<sub>n</sub> Implicit, Multifield, Multicomponent, Eulerian, Recriticality) is a computer code being developed at the Los Alamos Scientific Laboratory for the assessment of hypothetical core disruptive accidents in Liquid Metal Fast Breeder Reactors (LMFBR). Scenarios for such accidents include the evolution of highly distorted, molten core geometries. SIMMER couples space and time dependent neutronics with two-dimensional multifield, multicomponent fluid dynamics. The fluid dynamic model is based on that used in the KACHINA[2] program, in which the relative motion of two fields, liquid and vapor, is calculated using the Implicit Multifield (IMF) method. The KACHINA model has been extended in SIMMER by the addition of a structure field to model solid components. The coupled mass, momentum, and energy equations, along with an equation of state, are solved numerically to yield the material motion and thermophysical state of the system under consideration. Within each field all materials, or components, move with the same velocity. The structure field is fixed on space and acts as an infinite momentum sink.

Exchange models are provided allowing phase change within a material, transfer of momentum among the fields, and transfer of heat among the various components. The combined experimental and analytical program described here was undertaken in order to evaluate and, if necessary, modify

the model for momentum coupling between the vapor and liquid fields. The model assumes a dispersed flow regime, i.e., a continuous vapor phase with dispersed liquid droplets or solid particles. Solid particles are treated as a part of the liquid field.

## EXPERIMENT DESCRIPTION

The experimental apparatus consists in part of a vertical tubular glass column through which air is passed at known flow rates (see Fig. 1). Initially, a bed of solid, spherical particles rests on a fine mesh screen at the bottom of the tube. A flow straightening section to minimize circumferential motion (swirling) of the gas is located in the entry section below the screen. As gas is passed through the particles, they are fluidized. Flow conditions, such as air flow rate, initial bed depth, and particle size and density are varied, and the behavior of the bed is recorded. For the flow conditions studied in this work, the behavior of the bed is primarily a periodic slug flow or aggregate fluidization. An oscillatory period begins with the bed lifting off of the screen as a uniform mass. As it rises, it becomes more diffuse, and particles begin to drop off of the bottom collecting on the screen forming the next slug. The upper boundary of the rising slug remains relatively flat. When the interparticle distance becomes great enough and the local fluid velocity is not sufficient to support the particles, the remaining slug falls, joining the lower slug as it is lifting off the screen.

To facilitate correlation between the calculations and experiments, the following diagnostics were employed; (a) motion pictures to record qualitative behavior and maximum slug height (b) a differential pressure gauge across the column, and (c) a multibeam gamma to measure void fraction versus time for a given axial location. A schematic of the multibeam gamma densitometer and the accompanying data recording system is included in Fig. 1. Only two of the six channels were used for the reported measurements. The gamma sources were  $\frac{1}{2}$  mCi  $Ba^{137}$  sources and the detectors were NaI (Tl) scintillator/PM tubes. Each source was collimated to view a 25 mm axial length across the entire 67 mm inside diameter of the column. Discriminator levels were set to center on the 80 keV peak. During the experiment the mass distribution at any point along the tube is changing in time, producing a corresponding change in the count rate from each detector and a variation in the differential pressure across the bed. These signals are brought into a PDP/8I computer and recorded simultaneously. For the gamma detector channels, the total number of counts ( $\sim 10^3$ ) in successive 20 ms long time bins is recorded for up to 1024 time bins (20.5 s). For the differential pressure measurement, the 0-10 V signal corresponding to a pressure of 0.01 to 100 torr is converted into a digital signal by an analog-digital converter and then handled in a fashion similar to the detector channels.

Both the gamma signals and differential pressure gauges, examples of which are shown in Figs. 2 and 3, clearly indicate the periodic nature of the flow pattern. Each oscillation is not identical, however. In an experiment, for

a given flow condition, the period may vary as much as 30% from one slug to the next, and the slug height may vary as much as 40%. Averaged over several cycles (~25), however, the period and slug height are very repeatable for a given set of conditions. Because slug height is more variable and because period is the simpler characteristic to measure, average period was chosen as the primary characteristic measured in the experiments, and maximum slug height observed only casually.

Experiments were carried out using 3, 4, and 6 mm diameter soft glass beads (density = 2200 kg/m<sup>3</sup>) and 3 mm diameter aluminum spheres (density = 2700 kg/m<sup>3</sup>). Superficial vapor velocities were varied between 2.5 and 3.25 m/s, and the initial bed depth was varied between 0.12 and 0.20 m. Density measurements performed on the particle beds indicated that their initial packing density varied between 60 and 65% of theoretical. Clear variations in average oscillation period and peak height with superficial flow velocity, initial bed depth, and particle size and density were observed. Since the motion was not identically repeatable, the period was averaged over 100 oscillations. As one would expect, slug period increased with the strength of the vapor-particle interaction and the mass of the bed. The experimental data is summarized in Table I. The higher vapor velocity results in a longer oscillation period. A greater initial bed depth also produces a longer period. Surprisingly, no clear correlation emerges between period and particle radius. The heavier aluminum spheres have a longer oscillation period than do the glass beads. These results will be discussed in more detail along with analytical results in a later section.

#### SIMMER INTERFIELD DRAG MODEL

The following simplified liquid and vapor momentum equations illustrate the use of the momentum exchange coefficient  $K_{g\ell}$  as used in SIMMER.

#### LIQUID MOMENTUM EQUATION

$$\frac{\partial (\bar{\rho}_\ell V_\ell)}{\partial t} + \nabla \cdot (\bar{\rho}_\ell V_\ell V_\ell) = -\alpha_\ell \nabla P + g \bar{\rho}_\ell - K_{g\ell} (V_\ell - V_g) \quad (1)$$

#### VAPOR MOMENTUM EQUATION

$$\frac{\partial (\bar{\rho}_g V_g)}{\partial t} + \nabla \cdot (\bar{\rho}_g V_g V_g) = -\alpha_g \nabla P + g \bar{\rho}_g + K_{g\ell} (V_\ell - V_g) \quad (2)$$

where

$\bar{\rho}_g$  and  $\bar{\rho}_\ell$  are smear densities of vapor and liquid respectively,

$V_g$  and  $V_\ell$  are vector velocities of vapor and liquid respectively,

$\alpha_g$  and  $\alpha_l$  are volume fractions of vapor and liquid respectively,

P is local pressure,

g is gravitational acceleration, and

t is time.

The exchange term  $K_{gl}$  in the liquid equation represents the drag that is imposed on the liquid by the vapor. The drag model in SIMMER is based on flow of dispersed particles or droplets in a vapor field. When acceleration effects can be ignored the force on a particle in such a system is usually represented as a product of the dynamic pressure of the vapor stream, the projected area of the particle A, and a drag coefficient C

$$F = C \frac{\rho_g |V_g - V_l|^2 A}{2} \quad (3)$$

In this general form C includes the effect of both viscous and pressure contributions, as well as particle interaction effects in a multiparticle system. For the SIMMER formulation as in Eqs. (1) and (2) force is calculated per unit volume and the following expression for  $K_{gl}$  results

$$K_{gl} = \frac{3}{8} C \frac{\bar{\rho}_g \alpha_l}{\alpha_g r} \Delta V \quad (4)$$

The drag model used in KACHINA and initially used in SIMMER employs the following expression for C

$$C = \frac{1}{\alpha_g} \left( \frac{24}{Re} + C_D \right) \quad (5)$$

where

$$Re = \text{Reynolds number} = \frac{2r |V_g - V_l|}{\nu} \quad (6)$$

r = particle or droplet radius,

$\nu$  = kinematic viscosity, and

$C_D$  = form drag coefficient (input constant).

The  $1/\alpha_g$  term is included to account for multiparticle effects. The first term in the parenthesis is the viscous shear and the second is to account for pressure drag.

## SIMMER ANALYSIS

The calculational mesh used for the analysis is shown in Fig. 4. It is one dimensional with radial and angular symmetry. Both the bottom and top have constant pressure boundary conditions, the bottom having the higher pressure driving the gas flow. The lower-most cell contains only gas and is included as a plenum, simulating the piping in the experiment. The next cell which contains mostly structure serves two purposes. First, the gas-structure friction in this region can be varied controlling the pressure drop and thus the flow rate. Secondly, since the gas velocity is considerably greater in this region than elsewhere, it acts as a screen, preventing particles from dropping down into the plenum. The remainder of the cells contain vapor and/or particles and simulate the glass tube.

A base case problem was set up to run with the standard version of SIMMER. For this case, the 3 mm diameter soft glass beads at an initial bed depth of 0.16 m and a gas superficial velocity of 3 m/s was chosen. The calculation began with the particle bed at rest on the screen with no flow. Within about one half second (real time), a steady velocity profile had been established. By about one second a fairly repeatable oscillatory chugging motion had been set up. Qualitatively, the calculated motion of the particle bed was very similar to that observed experimentally, but the period and peak slug height were both significantly lower. The experiment had yielded a period of 0.9 s and a slug height that varied between 0.8 and 1.2 m. The calculated period was about 0.6 s and a maximum slug height of 0.45 m. It was apparent that the vapor-particle coupling was not strong enough and that another drag correlation should be considered.

A correlation was sought in which the drag coefficient  $C$  was calculated based on local material properties and flow conditions. It was also felt that the  $\frac{1}{\alpha_g}$  term in Eq. (5) may not adequately account for multiparticle effects. A literature search revealed the following formulation[3]

$$C = \frac{24}{\alpha_g^n Re_s} (1 + 0.15 Re_s^{0.687}) \quad , \quad (7)$$

where the Reynolds number  $Re_s$  is based on the superficial vapor flow velocity. The exponent  $n$  on the void fraction term is given as 4.7 in reference [3]. As this correlation addressed the weaknesses identified with Eq. (5), a trial version of SIMMER was produced in which it was incorporated. It was coded such that the index  $n$  could be selected as an input variable.

A series of calculations was performed using this version of SIMMER and the base case conditions described earlier. The index  $n$  was varied between 2 and 5. The results indicated that, at least for the base case, much better agreement between experiment and analysis could be had using the modified drag formulation. It must be noted, however, that if a value of  $n$  is chosen such that the calculated period is obtained, the resultant peak slug height

is greater than that experimentally observed. It was felt, however, that using Eq. (7) with the value 4.7 for  $n$  yielded acceptable agreement with the experiment for this particular case, and that this correlation would be used in analyzing the rest of the data.

Cases were run spanning the material and flow conditions used in the experiments. The results are shown compared to the experimental values in Figs. 5 through 7. Note first, that the calculated period for the base case, i.e., glass beads, 3 m/s vapor velocity, is 8% higher than the experimental value. The calculation of longer periods with higher flow rates does follow the experimental trend. The calculated period for the aluminum beads falls right on the experimental value. This combination of results is surprising. Since the SIMMER formulation treats both cases in a consistent manner one would expect a consistent deviation between experiment and calculation. Figure 6 shows the calculated and experimental variation of period with initial bed depth for the 3 mm glass beads. Again, the period is overcalculated, but the trend of increasing period with bed depth is consistent. Figure 7 shows the calculated and experimental periods for the three sizes of glass beads. As noted before, no clear trend is seen in the experimental results, but a decreasing period with increasing size is seen in the calculated cases. This result is reasonable if drag and gravity are the only forces acting on the beads. The gravitational forces on all beads should be the same, but the drag would be higher on the smaller beads resulting in a longer period.

## DISCUSSION OF RESULTS

Summarizing the analytical results, SIMMER accurately calculated the period for the single test with aluminum spheres. It over predicted the period for the 3 mm glass beads and under predicted the periods for the 4 and 6 mm glass. Several effects may be acting to cause this discrepancy. First of all, SIMMER is a finite difference code in which the equations of motion are solved only approximately. Some numerical error is inevitable. One calculation was performed for the base case (3 mm glass, 3 m/s, and 160 mm initial bed depth) in which the mesh size and time steps were cut by 50%. The resulting period was the same as in the standard cases. Another source of error introduced in the analysis is that SIMMER is not treating the solid spheres as rigid bodies. The calculation does not sense if the particles pack to a density greater than is possible in a solid particle system. This effect is minimized by the fact that the calculated drag force is a very strong function of void fraction. If the system begins to overpack, the drag force tends to force it open. Overpacking does result in a higher calculated drag than the real particle would see which might contribute to the overestimation of period for the 3 mm beads. This effect is not believed to strongly effect the calculation since void fractions less than 30% are never observed in the analysis and spherical particles may pack as tightly as 74% of their theoretical densities. A final potential source of error in the analysis is the drag formulation itself (Eq. (7)), and the manner in which it is coupled to the momentum equations.

There are also sources of uncertainty in the experimental results. The base case was tested in a tube that was 25% smaller than the standard apparatus. The resulting period was nearly 10% lower than the 0.89 s used for comparison. Evidently multidimensional effects are active. Since the experiment apparatus was not amenable to enlargement, the effect of using a larger tube was not studied. Other factors such as variation in particle size and shape and perhaps static electricity may be active. The lack of an experimental trend of shorter periods with larger glass bead diameter seems to indicate this fact. In the future, experiments will be performed with aluminum spheres of various sizes since they tend to be more uniform than glass and would be less effected by static electricity.

#### SUMMARY AND CONCLUSIONS

A series of aggregate flow fluidization experiments were performed. The observed oscillation periods were compared to those calculated by the SIMMER computer code. Initial analytical results indicated that the calculated momentum coupling between the vapor and particles was too weak. A different vapor-particle drag correlation was incorporated into the code, resulting in better agreement between experimental and calculated results.

Most calculations performed with SIMMER involve a large number of uncertainties. One of which is the validity and applicability of models used in the code for the particular thermophysical regime of interest. Considering the number and variety of other uncertainties, including the prediction of droplet size and distribution, it is felt that the vapor-particle/droplet drag model, modified as described here is adequate for most SIMMER applications. When calculations are performed in which the dispersed flow assumption is obviously not valid and the results are sensitive to the interfield drag treatment, a different correlation should be considered.

#### REFERENCES

1. L. L. Smith, "SIMMER-II: A Computer Program for LMFBR Disrupted Core Analysis," Los Alamos Scientific Laboratory report NUREG/CR-0453 LA-7515-M (October 1978).
2. A. A. Amsden and F. H. Harlow, "KACHINA: An Eulerian Computer Program for Multifield Fluid Flows," Los Alamos Scientific Laboratory report LA-5680 (December 1974).
3. Graham B. Wallis, One-Dimensional Two-Phase Flow (McGraw-Hill Book Company, New York, 1969) Chapter 8.

TABLE I  
EXPERIMENTAL RESULTS

<u>Bead Material</u>	<u>Particle Diameter, mm</u>	<u>Superficial Vapor Velocity m/s</u>	<u>Initial Bed Depth, mm</u>	<u>Oscillation Period, s</u>
Glass	3	2.5	160	0.72
Glass	3	3.0	160	0.89
Glass	3	3.25	160	0.92
Glass	3	3.0	120	0.71
Glass	3	3.0	200	1.02
Glass	4	3.0	160	0.96
Glass	6	3.0	160	0.96
Aluminum	3	3.0	160	0.94

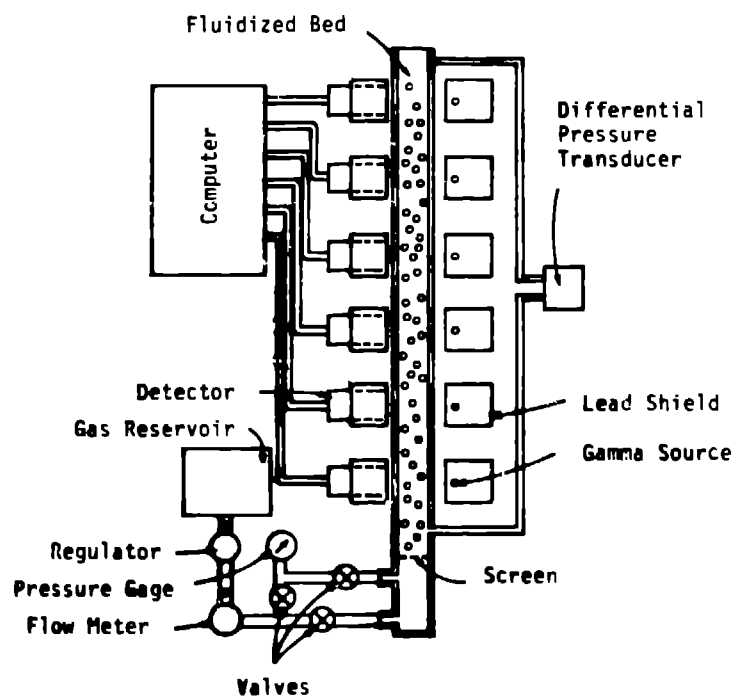


Fig. 1. Apparatus for interfield drag experiment.

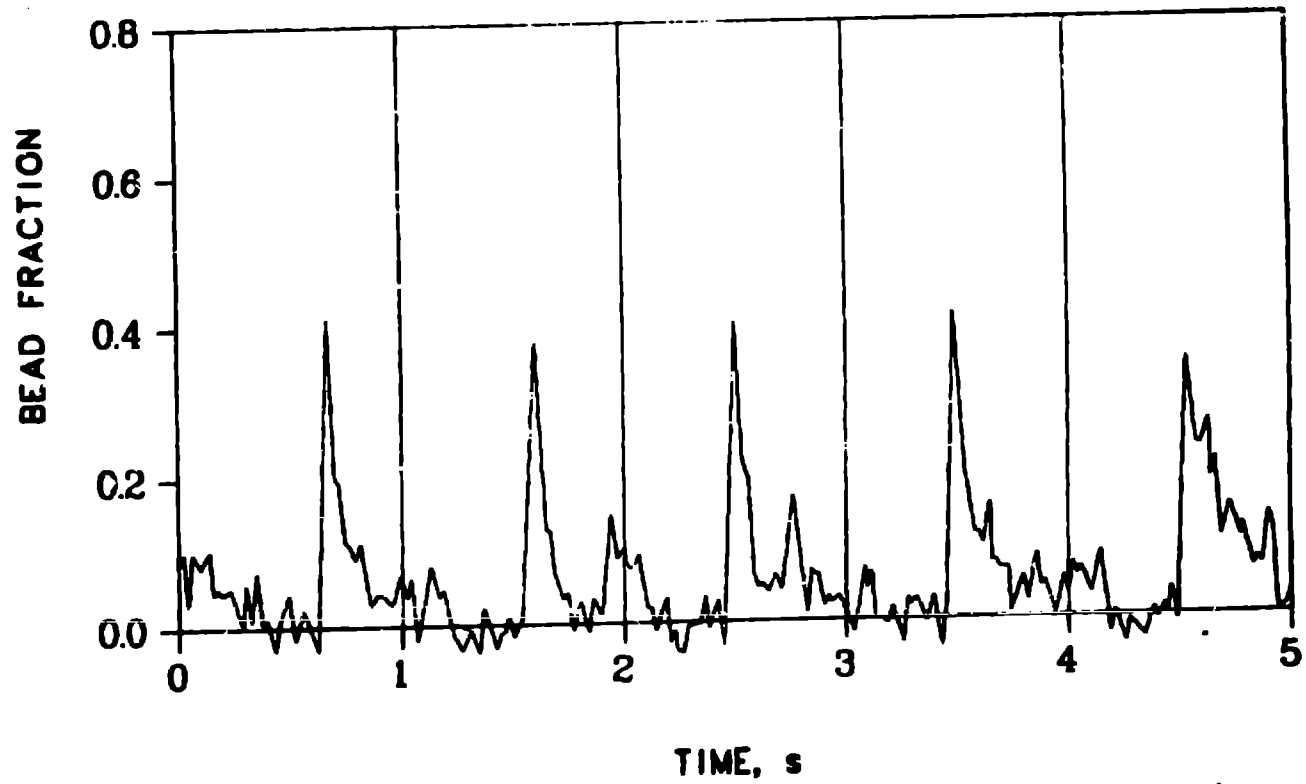


Fig. 2. Typical gamma densitometry data, showing particle fraction vs time.

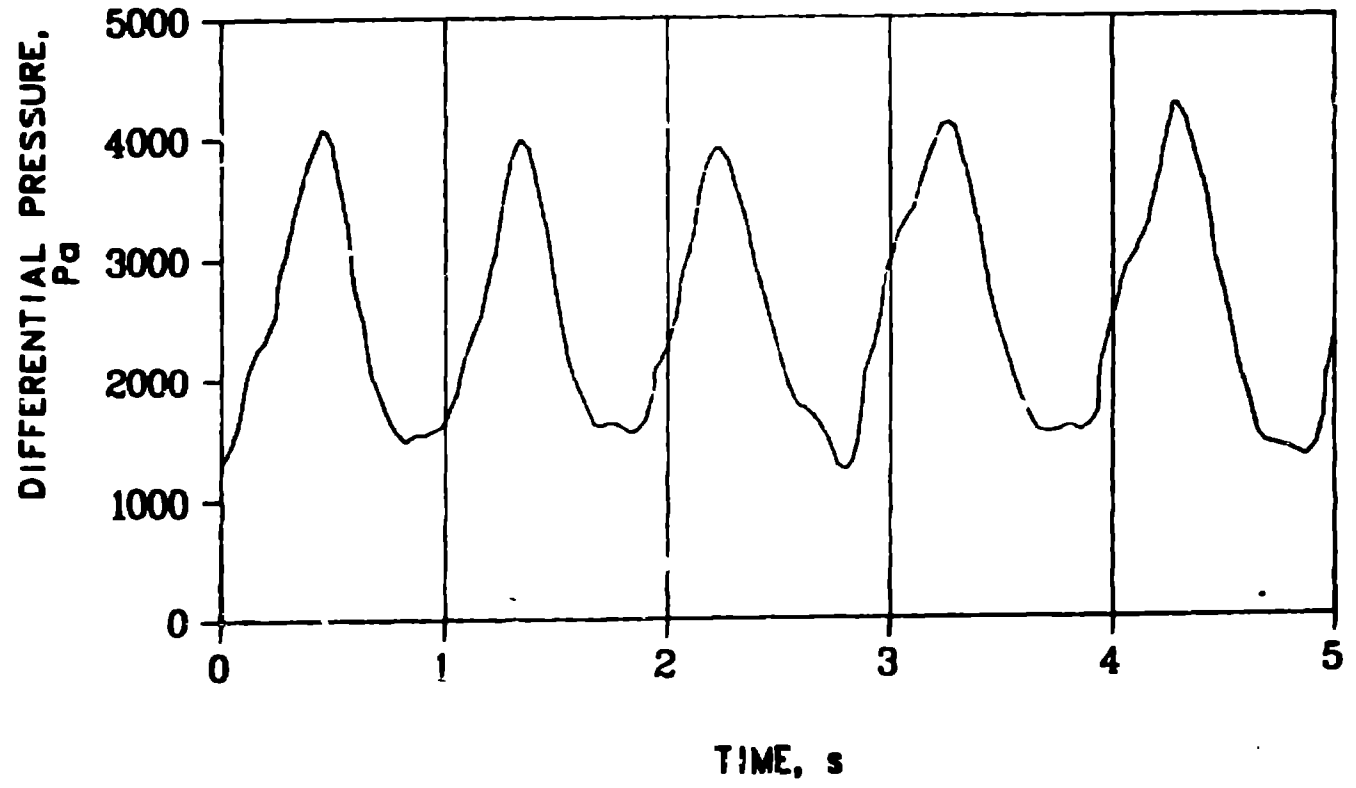


Fig. 3. Typical pressure transducer data, showing pressure drop across the bed vs time.

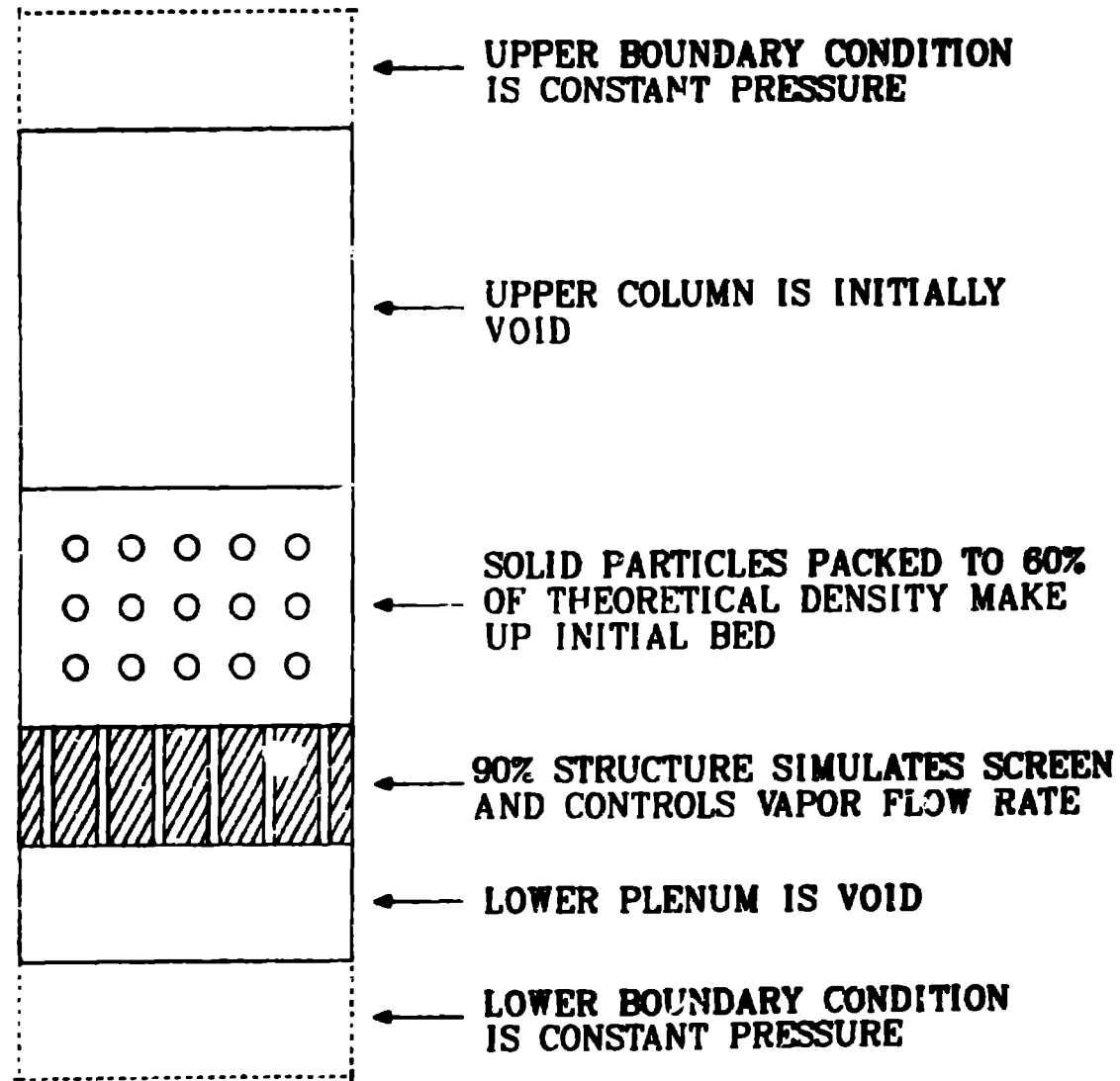


Fig. 4. Calculational mesh.

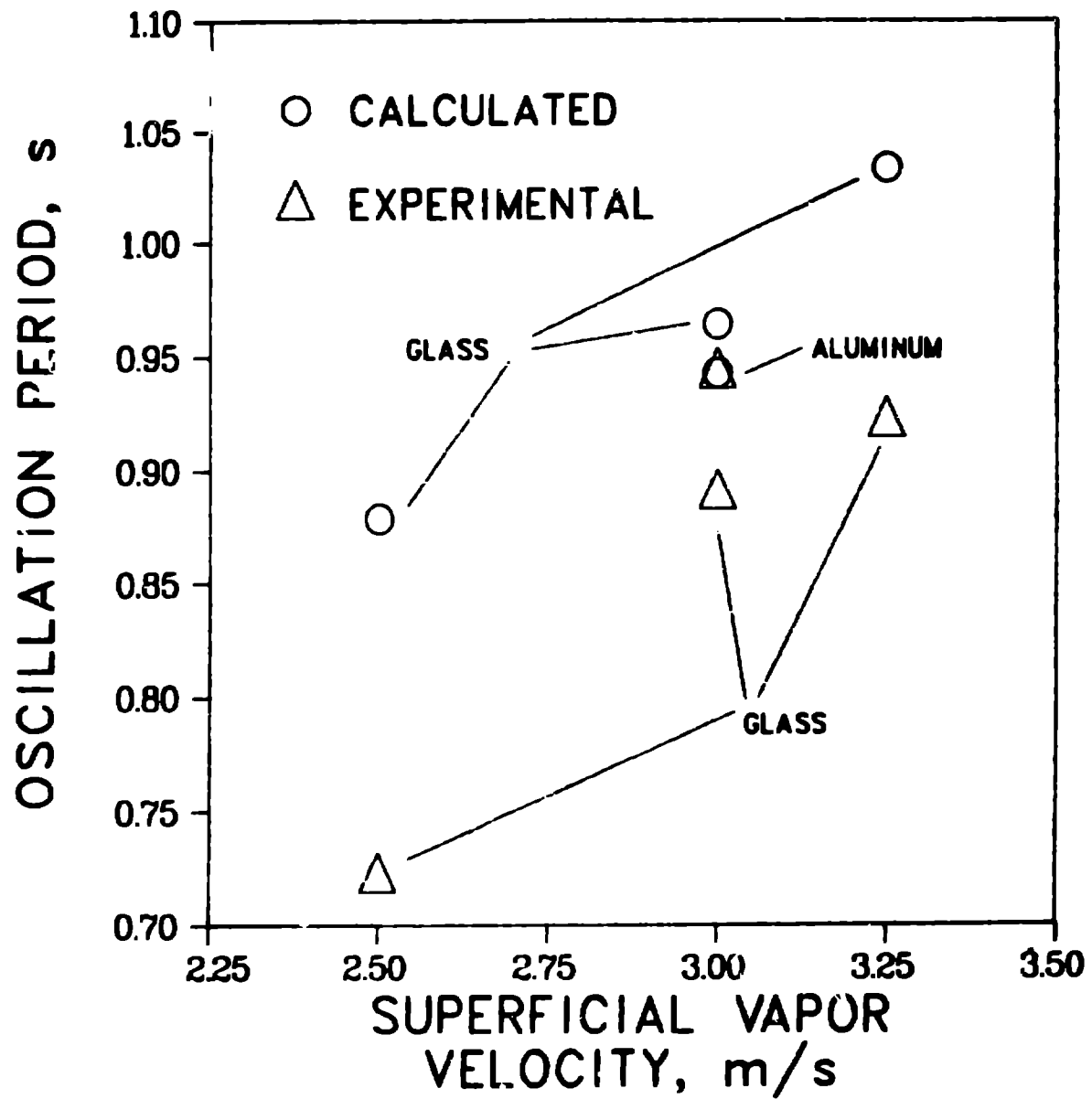


Fig. 5. Period vs vapor velocity for initial bed depth of 0.16 m.

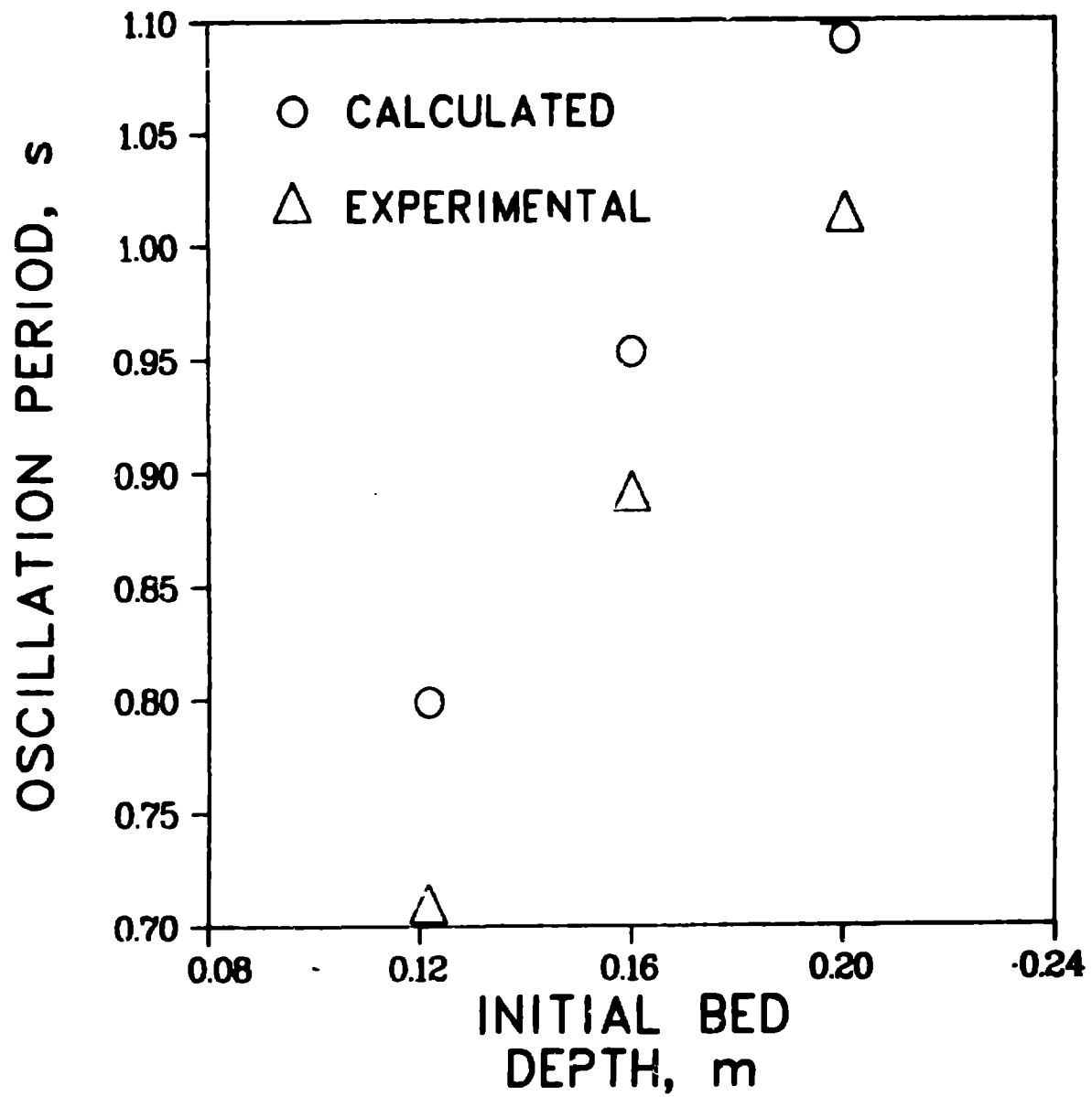


Fig. 6. Period vs initial bed depth for 3 mm diameter glass beads.

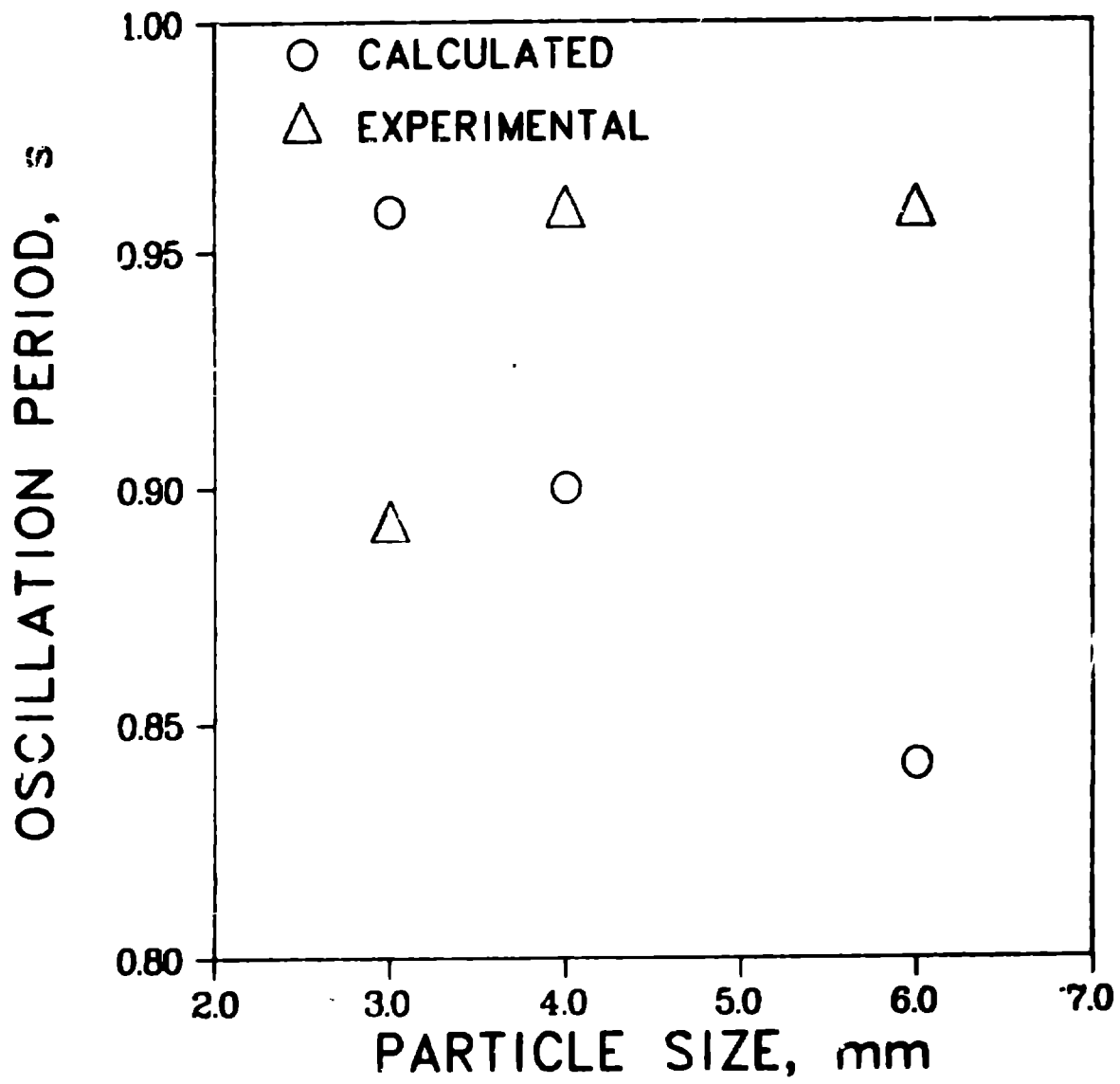


Fig. 7. Oscillation period vs size of glass beads.